



# Mathematical modelling of a tidal power station with diesel and wind units

Alexander Baykov, Andrey Dar'enkov, Andrey Kurkin\*, Elena Sosnina

Nizhny Novgorod State Technical University n.a. R.E. Alekseev, Russia

## ARTICLE INFO

### Article history:

Received 23 October 2018

Accepted 17 January 2019

Available online 21 January 2019

### Keywords:

Mathematical model  
Tidal power station  
Diesel generator  
Wind power unit  
Synchronous machine  
Power indices

## ABSTRACT

Hybrid power plants with renewable sources, having different frequencies and voltages of generated electricity, require coordination of its parameters on the basis of semiconductor converters. This causes the appearance of current and voltage harmonics in the electrical network. Analysis of the power characteristics of a hybrid power plant based on mathematical modeling will allow one to properly develop the power plant structure and select the parameters of the individual elements of its power part and control system. The article is devoted to the application of mathematical modeling for the analysis of the generated energy quality of a tidal power station with auxiliary diesel and wind units. The mathematical models for the analysis of the power indices of a tidal power station with diesel-wind aggregates are presented. Various designs of a power electrical part based on power electronic converters of electric power parameters having a microprocessor control system are considered. A detailed possibility analysis of the tidal aggregates operating modes is illustrated.

© 2019 The Authors. Production and hosting by Elsevier B.V. on behalf of King Saud University. This is an open access article under the CC BY-NC-ND license (<http://creativecommons.org/licenses/by-nc-nd/4.0/>).

## 1. Introduction

The development of world energy in the XXI century involves an active use of renewable energy: mechanical wind energy and water flows, thermal and radiant energy of solar radiation and heat of the Earth, chemical energy contained in biomass (Twidell and Weir, 2015; Ivannikova et al., 2015). Renewable energy sources are still inferior to traditional sources in terms of cost and scale of production, but this difference is steadily decreasing with its development (Ellabban and Abu-Rub; Blaabjerg, 2014; REN21, 2017).

Marine energy resources (Ocean Energy Forum, 2015) have huge reserves of energy – solar radiation absorbed by water, kinetic energy of sea waves (Contestabile et al., 2015; Falnes, 2007), currents, tides (Tidal Energy, 2014) and surf. At present there are spheres of their economically profitable use – when replacing diesel generators that supply electric power to autonomous consumers on islands, along a remote coastal zone, etc.

Despite the lack of potential energy resources of the seas and oceans, these technologies have not yet received its wide use. Their intensive application is hampered by natural shortcomings: large capital costs, intermittent and random nature of energy generation (Moghadasi et al., 2016; Gorji-Bandpy et al., 2013; Kocaman et al., 2016). Therefore, wave, tidal and other marine power plants are connected to centralized electrical networks (Li et al., 2015). In case of an autonomous operation, just in parallel with them, batteries (Maheshwari et al., 2017) or aggregates based on other sources of renewable energy, (usually wind and solar) are functioning (Wan et al., 2018; Powell et al., 2017).

Mathematical and computer modeling is widely used for the study of such complexes.

Many scientific papers are devoted to the modeling of tidal power plant components. The task of improving energy conversion aggregates is solved in (Renzi et al., 2013; Devolder et al., 2018; Mustafa et al., 2017). The tidal turbine modeling and fault diagnosis is carried out in MATLAB/Simulink in (Zhang et al., 2016). The paper (Ghefiri et al., 2018) deals with the modeling and control of a tidal stream generator for marine renewable energy. The paper (Li et al., 2011) focuses on the hydrodynamic performance of different forms of the duct which could accelerate the velocity of tidal flow.

The scientific papers devoted to modeling the entire system of a tidal power plant contribute to the solution of the problem. Mathematical modeling provides an opportunity to analyze energy and

\* Corresponding author.

E-mail address: [aakurkin@gmail.com](mailto:aakurkin@gmail.com) (A. Kurkin).

Peer review under responsibility of King Saud University.



other technical and economic indicators. In particular, a variable nature of the frequencies and voltage levels of the generated electric power necessitates the coordination of its parameters with the use of power electronic converters. But they, in their turn, can worsen the harmonic composition of currents and voltages (Vujacic et al., 2017; Bierhoff et al., 2008). The effect of the variation in tides on the power quality in stand-alone network is illustrated via simulation in (Aboul-Seoud et al., 2010).

Papers on the modeling of hybrid generation systems can be referred to a separate group. The paper (Aboul-Seoud et al., 2010) studies a network presenting a rural load, such as a small village, fed from a hybrid wind/tidal turbines that are connected to a weak grid. The paper (Tekobon et al., 2016) deals with the development of real time simulation for a hybrid wind – tidal power system.

It is necessary to work out technical solutions, both in the structure of power plants, and in the choice of the parameters of individual units and elements of the power part and control. Thus the authors have presented the results of the development of a mathematical modeling environment for a wind-diesel power station (Baykov et al., 2018), which are supplemented by a tidal aggregate with the operating modes and efficient analysis methods.

**2. Methods**

To analyze various electromechanical and electromagnetic processes in autonomous power plants a structural scheme (Fig. 1) is adopted, including three energy generation channels – diesel (*d*), wind (*w*) and tidal (*t*) equivalent to an active-inductive three-phase load (*l*), a backup source on the battery (*Ac*) and the common dc bus (*dc*). Energy sources—a diesel *D*, a wind wheel *W* and a tidal

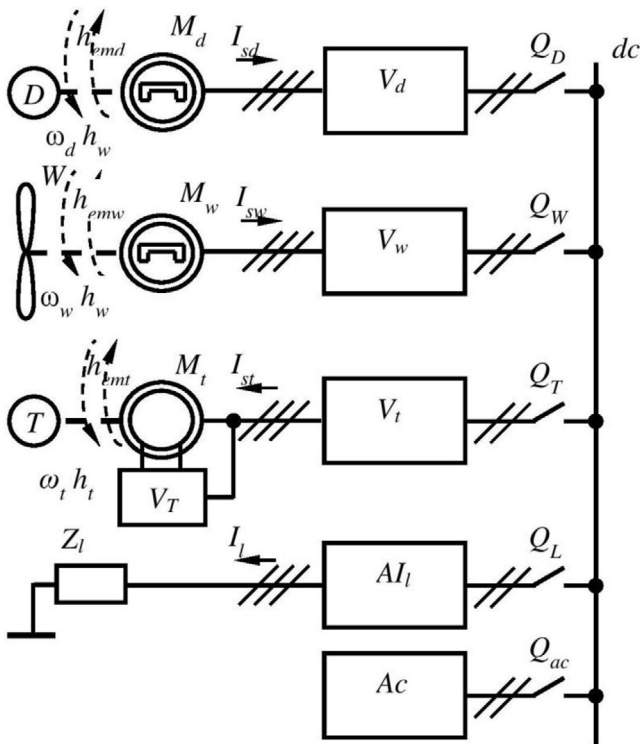


**Fig. 1.** Structural diagram of an autonomous power plant: *D*, *W*, *T* – diesel, wind wheel, turbine, *M<sub>d</sub>*, *M<sub>w</sub>*, *M<sub>t</sub>* – generators and *V<sub>d</sub>*, *V<sub>w</sub>*, *V<sub>t</sub>* – rectifiers of diesel generator, wind and tidal channels; *V<sub>T</sub>* – controlled rectifier excitation of the synchronous generator *M<sub>t</sub>*; *A<sub>l</sub>*, *Z<sub>l</sub>* – autonomous voltage inverter and equivalent load impedance; *Ac* – rechargeable battery; *Q* – switches; *dc* – bus direct current.

aggregate *T* rotate the shafts of the generators with frequencies  $\omega_d$ ,  $\omega_w$ ,  $\omega_t$ , developing the moments  $h_d$ ,  $h_w$ ,  $h_t$ . Instead of electromechanical energy converters, synchronous generators with permanent magnets (*M<sub>d</sub>*, *M<sub>w</sub>*) and *M<sub>t</sub>* – with a controlled exciter (*V<sub>T</sub>*) are used as an option.

Three-phase currents of stator generators (*I<sub>sd</sub>*, *I<sub>sw</sub>*, *I<sub>st</sub>*) are converted into constants by controlled and uncontrolled rectifiers (*V<sub>d</sub>*, *V<sub>w</sub>*, *V<sub>t</sub>*). The use of the uncontrolled rectifiers is explained by connecting an autonomous inverter to the output. Depending on the situation with the load demand, wind speed and the parameters of the tidal channel, the operator switches (*Q<sub>d</sub>*, *Q<sub>w</sub>*, *Q<sub>t</sub>*, *Q<sub>l</sub>*, *Q<sub>ac</sub>*) to make the various schemes of the power plant operation work.

The tidal channel, which is the main and the most powerful, for example 400 kW, like the Vislogub tidal power station (Forum et al., 2015), provides the operation in various turbine and pumping modes. To generalize, a direct pumping mode of the tidal aggregate is of interest. It works as an asynchronous motor and operates the pump to take water from the sea into the basin which stores energy. If we assume that at this time the consumption is 100 kW, and the capacity of the wind channel is 200 kW, then the power consumption of the tidal channel will be 100 kW. The tidal channel converter operates in the autonomous voltage inverter mode. Thus, the calculation scheme for reproducing processes in the power circuit (Fig. 2) is supposed to use mathematical models of the synchronous generator, the asynchronous motor, the rectifier and the autonomous voltage inverter, i.e. a fairly wide range of models of objects.

The mathematical model of the wind turbine is described in (Baykov et al., 2018).

To analyze the energy parameters of the circuit, it is possible to simplify the representation of the power electronic circuits, as ideal voltage converters of a three-phase alternating current to a constant one and back Khan et al. (2017). It is advisable to single out the influence of the processes of gates commutation on the shapes of currents and voltages in a separate problem and to carry out in private design schemes of a smaller size. Therefore, it is possible to describe the functioning of complex multi-circuit circuits with key elements by simple nodes based on the dependent current and voltage sources (*V<sub>w</sub>*, *A<sub>l</sub>*, *A<sub>l</sub>*).

**3. Results**

In the wind channel circuit, the uncontrolled rectifier *V<sub>w</sub>* switches valves in six sections on the EMF period of the generator *M<sub>w</sub>* in accordance with the values of the line voltages, thereby performing a functional conversion of the voltages *U<sub>cxw</sub>* at the rectifier input to the pulsating DC power supply

$$e_{V_w} = [X_V U_{cxw}]_{j_{max}}, \quad X_V = \begin{bmatrix} 1 & -1 & 0 \\ 1 & 0 & -1 \\ 0 & 1 & -1 \\ -1 & 1 & 0 \\ -1 & 0 & 1 \\ 0 & -1 & 1 \end{bmatrix}, \quad (1)$$

where *X<sub>V</sub>* is a topological matrix providing calculation of linear voltages at the output of the three-phase bridge rectifier; *j<sub>max</sub>* is the number of the line corresponding to the maximum value of the vector *X<sub>V</sub>U<sub>cxw</sub>*. The capacitances *C<sub>xw</sub>* correspond to either the filter capacitors, if present in the actual circuit, or to the specially introduced capacitances of the stator coupling circuit of the machine and the controlled external circuit. In both cases, it connects in parallel the coupling resistance *r<sub>xw</sub>* of a large value, which matches the stator circuit of the machine and the rectifier input circuit by determining the ratio between the currents

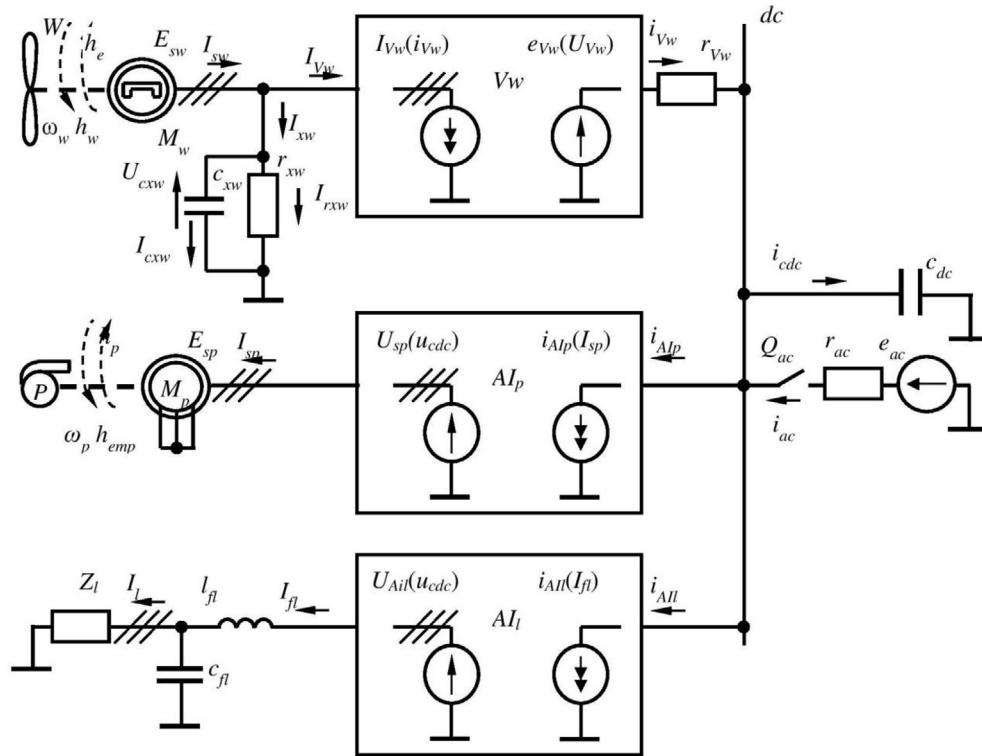


**Fig. 2.** The design scheme of an autonomous power plant with power from the wind channel of a load and a tidal unit operating in the mode of a direct pump:  $W, P$  is a wind and a pump,  $M_w, V_w$  is a synchronous generator with permanent magnets and a wind channel rectifier,  $M_p$  – is a tidal channel machine operating in an asynchronous motor mode;  $AI_p, AI_l$  – autonomous voltage inverters of the tidal channel and load circuit;  $Z_l$  is the equivalent impedance of the load circuit  $r_{xw}, r_{vw}, c_{xw}$  – active resistances and capacities of communication circuits;  $l_p, c_{fl}$  – inductance and capacity of the load filter;  $Q_{ac}, r_{ac}, e_{ac}$  – switch, resistance and EMF (Electromagnetic field) of the battery;  $dc$  – dc bus with  $c_{dc}$  capacity.

$$I_{cxw} = I_{sw} - I_{Vw} - r_{xw}^{-1} U_{cxw}. \quad (2)$$

The vector of the stator currents of the generator  $I_{Vw}$ , is assumed to be dependent on the output current of the rectifier and is determined by a similar functional transformation

$$I_{Vw} = [X_V i_{Vw}]_{j_{max}} \quad (3)$$

based on the choice of the string  $j_{max}$  from the vector  $X_V i_{Vw}$ . In its turn, the output of the rectifier is switched on by a small resistance  $r_{Vw}$ , so that the rectifier circuits  $V_w$  and DC  $dc$  are matched:

$$i_{Vw} = r_{Vw}^{-1} (e_{Vw} - u_{cdc}). \quad (4)$$

The capacity of  $cdc$  can be present in the circuit as a filter element, or it should be included artificially with a small parameter value.

The consumed input currents ( $i_{AIp}, i_{AIl}$ ) of the units of the autonomous pump inverters of the tidal aggregate and the equivalent load are determined by the stator  $M_p$  currents  $I_{sp}$  and  $I_{fl}$  and the load circuit filter inductances

$$\begin{aligned} i_{AIp} &= \text{diag}[x_{p1} \quad x_{p3} \quad x_{p5}] I_{sp}, \\ i_{AIl} &= \text{diag}[x_{l1} \quad x_{l3} \quad x_{l5}] I_{fl}, \end{aligned} \quad (5)$$

where the diagonal matrix is composed of the values of the control functions of the transistors of the odd or even group of the three-phase bridge circuit. It is assumed that if a control pulse is available, the value of the corresponding function is equal to one, otherwise it is zero. The definition of these functions is determined on the well-known vector control algorithm based on the principle of pulse width modulation.

According to the law of frequency control, the amplitudes of the voltage vector components  $U_{AIp}$  on the stator of the  $M_p$  machine

operating in the asynchronous motor mode, depend on the frequency  $f_{sp}$  of the generated voltage

$$u_{AIp} = \sqrt{2} \frac{u_{snom} f_{sp}}{f_{snom}} = \frac{u_{smax} f_{sp}}{f_{snom}}, \quad (6)$$

where  $u_{snom}, f_{snom}$  is the nominal effective value and frequency of the phase voltage of the machine. Similarly, the frequency of the load voltage  $f_l$  is the amplitude of the voltage vector  $U_{AIl}$

$$u_{AIl} = \sqrt{2} \frac{u_{nom} f_l}{f_{lnom}} = \frac{u_{max} f_l}{f_{lnom}}. \quad (7)$$

The rotation of the vectors  $U_{AIp}$  and  $U_{AIl}$  with the corresponding angular frequencies  $\omega_p$  and  $\omega_l$  occurs in six sectors. The position of the formed vector of length  $u_{AIj}$  ( $j = p, l$ ) is determined within the

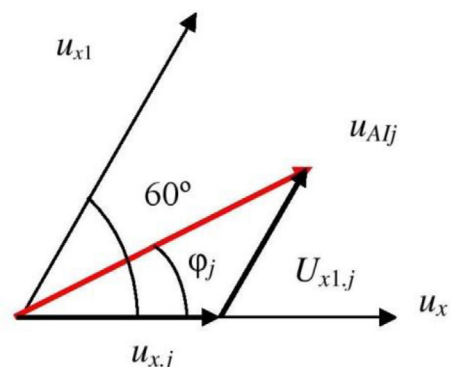


**Fig. 3.** Formation of the current position of the voltage vector.

current sector by the  $k_{sect}$  angle  $\varphi_j$  (Fig. 3). This angle is calculated at discrete instants of time  $t_n$ , counted in units of measurement of simulation time and coinciding with the modulation cycles,

$$\varphi_j = \frac{2\pi\omega_j(t_n - t_{nj})}{T_j} - (k_{sect} - 1) \frac{\pi}{3}, \quad (8)$$

where  $t_{nj}$  is the time instant corresponding to the beginning of the reproduced period  $T_j$  of the frequency voltage  $f_j$ .

The ratio of the generating vector lengths  $u_{xj}$  and  $u_{x1j}$  to the base vector lengths

$$u_{Bj} = \frac{2}{3} u_{maxj} = \frac{2}{3} u_{xj} = \frac{2}{3} u_{x1j} \quad (9)$$

determines the duty cycle

$$\gamma_{xj} = \frac{u_j}{u_{Bj}} \frac{(\cos\varphi_j - \sin\varphi_j)}{\sqrt{3}}, \quad \gamma_{x+1j} = \frac{u_j}{u_{Bj}} \frac{2\sin\varphi_j}{\sqrt{3}}. \quad (10)$$

Using the rounding operation, we calculate the numbers of cycles  $k_{xj}$ ,  $k_{x1j}$  and  $k_{0j}$  for these vectors and for the zero interval within the  $T_{shim}$  PWM (Pulse width modulation) modulation period which consists of a number of cycles

$$k_{xj} = \text{round}\left(\frac{\gamma_{xj} T_{shim}}{dt_{tact}}\right), \quad k_{x+1j} = \text{round}\left(\frac{\gamma_{x+1j} T_{shim}}{dt_{tact}}\right), \quad k_{0j} = \frac{T_{shim}}{dt_{tact}} - k_{xj} - k_{x+1j}. \quad (11)$$

The generating vectors are formed by combinations of open and closed transistors that coincide with the combinations of control pulses  $X_j$  according to Table 1.

In the next calculation step, after determining the sector, the PWM period and the interval inside it, control pulse vectors  $X_j$  are set, which have already been used in (5) to calculate the input currents of the inverters. They are also used to calculate three-phase voltages at the output of the inverter of a tidal aggregate

$$\begin{aligned} U_{sp} &= 0, \text{ if } x_2 + x_4 + x_6 = 0, \\ U_{sp} &= 0, \text{ if } x_2 + x_4 + x_6 = 3, \\ U_{sp} &= (-diag(x_1 \ x_3 \ x_5) + \frac{2}{3})u_{cdc}, \text{ if } x_2 + x_4 + x_6 = 1, \\ U_{sp} &= (diag(x_2 \ x_4 \ x_6) - \frac{2}{3})u_{cdc}, \text{ if } x_2 + x_4 + x_6 = 2, \end{aligned} \quad (12)$$

where the values of the key management functions of the analyzed inverter are used, and in the case of the load channel, the stress vector indices the change from “sp” to “Ail”.

**Table 1**  
Formation of control pulses by sector intervals.

$k_{sect}$	Vectors	Pulses					
		$x_1$	$x_2$	$x_3$	$x_4$	$x_5$	$x_6$
1	X	1	0	0	1	0	1
	$X_1$	1	0	1	0	0	1
	$X_0$	1	0	0	0	1	0
2	X	1	0	1	0	0	1
	$X_1$	0	1	1	0	0	1
	$X_0$	0	1	0	1	0	1
3	X	0	1	1	0	0	1
	$X_1$	0	1	1	0	1	0
	$X_0$	1	0	1	0	1	0
4	X	0	1	1	0	1	0
	$X_1$	0	1	0	1	1	0
	$X_0$	0	1	0	1	0	1
5	X	0	1	0	1	1	0
	$X_1$	1	0	0	1	1	0
	$X_0$	1	0	1	0	1	0
6	X	1	0	0	1	1	0
	$X_1$	1	0	0	1	0	1
	$X_0$	0	1	0	1	0	1

An important advantage of the described algorithm for modeling vector control of autonomous voltage inverters is the speed that does not exclude accounting for discreteness not only in the modulation frequency of PWM (20 kHz), but also in clock frequency.

#### 4. Discussion

The functioning of electromechanical processes in the circuit (Fig. 2) is described on the basis of the application of the Park-Gorev coordinate transformations (Gorev, 1950). Equations of the state of a wind channel with neglect of the effect of compensating circuits in static modes

$$\begin{aligned} \frac{d}{dt} \psi_{dw} &= -\omega_{rw} \psi_{qw} - r_{sw} i_{dw} - u_{dcxw}, \\ \frac{d}{dt} \psi_{qw} &= \omega_{rw} (\psi_{dw} + \psi_{fw}) - r_{sw} i_{qw} - u_{qcxw}, \\ \frac{d}{dt} \omega_{rw} &= j_w^{-1} (h_w - h_{emw}), \\ \frac{d}{dt} \theta_{rw} &= \omega_w, \\ \frac{d}{dt} U_{cxw} &= C_{xw}^{-1} I_{cxw} \end{aligned} \quad (13)$$

have as independent variables:  $\psi_{dw}$ , and  $\psi_{qw}$  are flux linkages of a two-phase equivalent machine along the longitudinal transverse axis;  $\omega_w$  and  $\theta_w$  – are the rotational speed and rotational angle of the rotor,  $U_{cxw}$  – is the voltage vector of the capacitances of the communication circuit. The linkage of the permanent magnet of the rotor  $\psi_{fw}$  is a parameter. The right-hand sides of equation (13) are calculated using relations

$$\begin{aligned} I_{dqw} &= \begin{bmatrix} L_{dw}^{-1} & 0 \\ 0 & L_{qw}^{-1} \end{bmatrix} \begin{bmatrix} \psi_{dw} \\ \psi_{qw} \end{bmatrix}, \quad U_{dqxw} = \begin{bmatrix} u_{dxw} \\ u_{qxw} \end{bmatrix} = A_{dqw} \begin{bmatrix} U_{cxw.1} \\ U_{cxw.2} \end{bmatrix}, \\ h_{emw} &= 1, 5 i_{qw} \psi_{fw} \\ I_{sw} &= A_{dqw}^{-1} I_{dqw}, \quad I_{xw} = I_{sw} - I_{vw}, \quad I_{rxw} = r_{xw}^{-1} U_{cxw}, \quad I_{cxw} = I_{xw} - I_{rxw}, \\ A_{dqw} &= 2/\sqrt{3} \begin{bmatrix} \sin(\theta_{rw} + \pi/3) \sin(\theta_{rw}) \\ \cos(\theta_{rw} + \pi/3) \cos(\theta_{rw}) \end{bmatrix}, \end{aligned} \quad (14)$$

where  $L_{dw}$ ,  $L_{qw}$ ,  $r_{sw}$  – is the stator inductance of the  $M_w$  machine along the longitudinal and transverse axes and the active resistance of the stator winding;  $j_w$  – is the moment of inertia of the wind power unit.

A similar equation would be for the generator  $M_p$  of the channel of the tidal aggregate in the turbine mode. In the same mode of the

induction motor driving the pump, its equation of state has the form

$$\begin{aligned} \frac{d}{dt} \Psi_{dqsp} &= U_{dqsp} + \omega_{sp} B \Psi_{dqsp} - r_{sp} I_{dqsp}, \\ \frac{d}{dt} \Psi_{dqrp} &= (\omega_{sp} - \omega_{rp}) B \Psi_{dqrp} - r_{rp} I_{dqrp}, \\ \frac{d\omega_{rp}}{dt} &= j_{rp}^{-1} (h_{emp} - h_p), \\ \frac{d\theta_{rp}}{dt} &= \omega_{rp}, \end{aligned} \quad (15)$$

where  $\Psi_{dqsp}$ , and  $\Psi_{dqrp}$  are the stator and rotor flux linkages of the two-phase equivalent machine Mp along the longitudinal transverse axis;  $\omega_p$  and  $\theta_s$  – rotational speed and rotor angle. The right-hand sides of equation (15) are calculated using (12) and relations:

$$A_{dqsp} = 2/\sqrt{3} \begin{bmatrix} \sin(\theta_{sp} + \pi/3) \sin(\theta_{sp}) \\ \cos(\theta_{sp} + \pi/3) \cos(\theta_{sp}) \end{bmatrix}, \quad \theta_{sp} = \omega_{sp} t, \quad B = \begin{bmatrix} 0 & -1 \\ 10 & \end{bmatrix},$$

$$U_{dqsp} = A_{dqsp} \begin{bmatrix} u_{sp,1} \\ u_{sp,2} \end{bmatrix}, \quad I_{dqsp} = L_{srp}^{-1} \begin{bmatrix} \Psi_{dqsp} \\ \Psi_{dqrp} \end{bmatrix} = \begin{bmatrix} I_{dqsp} \\ I_{dqrp} \end{bmatrix} = \begin{bmatrix} i_{dsp} \\ i_{qsp} \\ i_{drp} \\ i_{qrp} \end{bmatrix},$$

$$L_{srp} = \begin{bmatrix} l_{sp} & 0 & l_m & 0 \\ 0 & l_{sp} & 0 & l_m \\ l_m & 0 & l_{sp} & 0 \\ 0 & l_m & 0 & l_{sp} \end{bmatrix},$$

$$h_{emp} = l_m (i_{qsp} i_{drp} - i_{dsp} i_{qrp}), \quad I_{sp} = H_1' A_{dqsp}^{-1} I_{dqsp}, \quad (16)$$

where  $l_{sp}$ ,  $l_{rp}$ ,  $r_{sp}$ ,  $r_{rp}$  – are the inductances and the active resistances of the stator and rotor windings of the  $M_p$  machine in the operating mode of the induction motor;  $j_p$  – is the moment of inertia of the tidal aggregate.

Equation of state of three-phase equivalent active-inductive load  $r_l$ - $l_l$ :

$$\begin{aligned} \frac{d}{dt} I_{hl} &= L_{hl}^{-1} (U_{hcf1} - R_{hl} I_{hl}), \\ \frac{d}{dt} I_{Al} &= l_{fl}^{-1} (U_{Al} - U_{hcf1} - r_{fl} I_{Al}), \\ \frac{d}{dt} U_{cf1} &= c_{fl}^{-1} (I_l - I_{Al}) \end{aligned} \quad (17)$$

has as independent variables the loop currents  $I_{hl}$  of the load circuit, the currents  $I_{fl}$  of inductances and the voltage of the capacitances  $U_{cf1}$  of the filter having the parameters  $l_{fl}$ ,  $r_{fl}$ ,  $c_{fl}$ . The right-hand sides of (17) are calculated taking into account (12) and relations

$$\begin{aligned} U_{chl} &= H_1 U_{cfload}, \quad I_l = H_1' I_{hl}, \quad H_1 = \begin{bmatrix} 1 & 0 & -1 \\ 0 & 1 & -1 \end{bmatrix}, \\ L_{hl} &= H_1 \begin{bmatrix} l_l & 0 & 0 \\ 0 & l_l & 0 \\ 0 & 0 & l_l \end{bmatrix} H_1', \quad R_{hl} = H_1 \begin{bmatrix} r_l & 0 & 0 \\ 0 & r_l & 0 \\ 0 & 0 & r_l \end{bmatrix} H_1'. \end{aligned} \quad (18)$$

The DC bus connecting the circuit channels has at least one inertial parameter – the capacitance  $c_{dc}$ , which can be a real capacitor filter battery, or an artificially introduced small communication capacitance. The equation of state of the voltage of this capacitance is expressed using the results of the calculation of the power supply EMF at the outlet of the wind channel (1) and the currents consumed by the pump channel of the tidal unit and the equivalent load (5):

$$\frac{du_{cdc}}{dt} = c_{dc}^{-1} (r_{vw}^{-1} (e_{vw} - u_{cdc}) - i_{Alp} - i_{All}) \quad (19)$$

An important stage in the analysis of the effectiveness of the technical solutions being adopted is the determination of integral indicators of the quality of the functioning of devices. For the analysis of the most important of them – energy indices a harmonic analysis of the curves of the functions  $F$  of the phase currents  $I_j$  and the voltage  $U_j$  is provided. When reproducing the corresponding processes, these curves are obtained as arrays from the values  $F_{j(n)}$  ( $n = 1, 2, \dots, N_{dt}$ ) on the period  $T$  with the same step  $dt$ . The harmonic components of the phase currents and voltages are found from the formulae:

$$\begin{aligned} F_{A,j(k)} &= \sum_{n=1}^{N_{dt}} F_{j(n)} \cos(k2\pi \frac{1}{T} n \cdot dt), \\ F_{B,j(k)} &= \sum_{n=1}^{N_{dt}} F_{j(n)} \sin(k2\pi \frac{1}{T} n \cdot dt). \end{aligned} \quad (20)$$

In the case of symmetry of the phase parameters, the index “j” can be omitted. It is assumed that the number  $N_k$  of harmonic components satisfies the condition:

$$\frac{N_{dt}}{N_k} \geq K_{min}, \quad (21)$$

where the required number of points for determining the harmonic  $K_{min} = 16 \div 20$ .

The components “A” and “B” compute the amplitudes and phases of the harmonics:

$$\begin{aligned} F_{max,j(k)} &= \sqrt{F_{Aj(k)}^2 + F_{Bj(k)}^2}, \\ \phi_{j(k)} &= \arctan \frac{F_{Aj(k)}}{F_{Bj(k)}}. \end{aligned} \quad (22)$$

The effective values of current and voltage are calculated as rms instantaneous values at a constant step:

$$F_{eff,j} = \sqrt{\frac{1}{N_{dt}} \sum_{n=1}^{N_{dt}} F_{j(n)}^2}. \quad (23)$$

The total electrical power consumed or delivered by the motor is found from the effective values of the phase currents and voltages:

$$S_{el} = \sum_{j=1,2,3} I_{eff,j} U_{eff,j}. \quad (24)$$

The active and reactive power consumed or delivered by the PMSM (Permanent magnet synchronous motor) are found from the first harmonic components of the phase currents and voltages (Maevskiy, 1978):

$$\begin{aligned} P_1 &= \frac{1}{2} \sum_{j=1,2,3} I_{max,j(1)} U_{max,j(1)} \cos(\varphi_{Uj(1)} - \varphi_{Ij(1)}), \\ Q_1 &= \frac{1}{2} \sum_{j=1,2,3} I_{max,j(1)} U_{max,j(1)} \sin(\varphi_{Uj(1)} - \varphi_{Ij(1)}). \end{aligned} \quad (25)$$

The power of asymmetry appears in the case of a phase-by-phase difference in the parameters of the load and is found from:

$$Q_3 = \frac{1}{\sqrt{2}} U_{eff,1} \sqrt{2 \sum_{j=1,2,3} I_{max,j(1)}^2 - \sum_{g,q=1,2,3} I_{max,g(1)} I_{max,q(1)} \cos(\varphi_{g(1)} - \varphi_{q(1)}), \quad g \neq q} \quad (26)$$

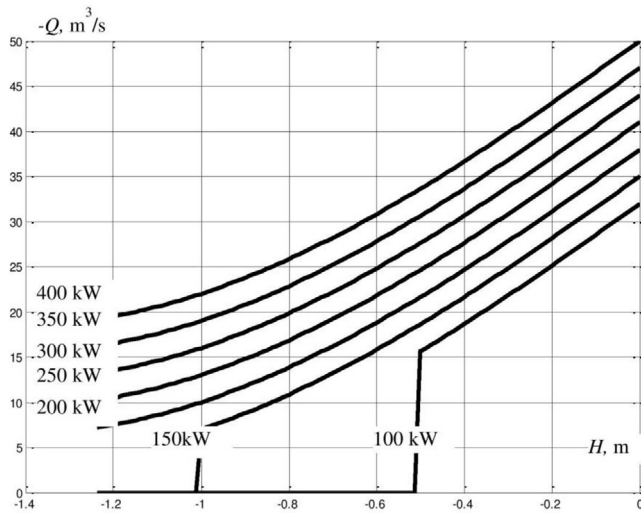


Fig. 4. Approximated discharge-pressure characteristics of the tidal aggregate Vislogubskaya TPS (Tidal power station) in the direct pump mode.

where from the sum of the squares of the amplitudes of the first harmonics of the phase currents, all possible combinations of products of these amplitudes are subtracted by the cosines of the differences in the angles of the lagging angles of the first harmonics of the currents from the voltages.

The distortion power consumed or delivered by the motor is found as a quadratic remainder of the total power:

$$Q_2 = \sqrt{S_{el}^2 - P_1^2 - Q_1^2 - Q_3^2}. \tag{27}$$

With the known values of the total power, its components, equivalent to the active resistance of the load, power, shear, distortion and useful factors are calculated.

Formulae for determining the power, shear, distortion, asymmetry and useful factors are:

$$k_M = \frac{P_1}{S_{el}}, \quad k_C = \sqrt{\frac{P_1^2}{P_1^2 + Q_1^2}}, \quad k_2 = \frac{\sqrt{P_1^2 + Q_1^2}}{\sqrt{P_1^2 + Q_1^2 + Q_2^2}}, \tag{28}$$

$$k_3 = \frac{\sqrt{P_1^2 + Q_1^2 + Q_2^2}}{S_{el}}, \quad \eta = \frac{3r_1 I_{eff}^2 + I_{emh} \omega_{rp}}{I_{emw} \omega_{rw}}.$$

The calculation of aggregate loads in real operational modes is necessary to ensure the reliability of the simulation results and is carried out with the use of the approximation of the available

technical characteristics of the units. In particular, for the diesel-generator channel, it is possible to use adjusting characteristics that establish the realizable relationship between the moment on the shaft and its speed (Baykov et al., 2018). For the tidal power plant assembly, the flow-pressure characteristics of the  $Q-H$  are approximated. For example, in the direct-pump mode at the Vislogub tidal power plant 400 kW [Bernshtein and Silakov, 1987, Fig. 6.1], the characteristic family of the water inflow from the sea into the pool is represented by the formula:

$$Q_p = \sum_{k=1}^4 q_{pk} H^{k-1}, \tag{29}$$

where for power, the values of the coefficients  $q_p = [-50 \ 35 \ -2 \ -5]$   $m^3/s$  at a power of 400 kW, and for smaller powers of  $q_p(1)$ , the value changes from  $-50$  to  $-32$  (Fig. 4). On the basis of the approximation dependences of the type (29), it is possible to determine programmatically the loads of force elements.

Previously mentioned the system operation mode with power from the wind channel, when the available excess capacity of 100 kW is used for pumping water into the pool. If the water level in it is 0.5 m above the sea level, then according to the characteristics (Fig. 4), the productivity will be 15  $m^3/s$ . For the mechanisms under consideration, the cubic dependence of the power and the quadratic moment on the rotational frequency are typical. Therefore, using the known nominal frequency values  $\omega_{0nomp}$ , and the power  $P_{pnom}$ , the required synchronous rotational speed  $\omega_{op}$  determining the parameters  $Al_p$ , and the corresponding torque  $h_p$  on the pump shaft for the mode with power  $P_p$ :

$$\omega_{op} = \omega_{0nomp} \sqrt[3]{\frac{P_p}{P_{pnom}}} = \omega_{0nomp} \sqrt[3]{\frac{100}{400}} = 0,63 \omega_{0nomp} = 0,63, \tag{30}$$

$$h_p = \frac{P_p}{P_{pnom}} \frac{\omega_{op}}{\omega_{0nomp}} = 0,25 \cdot 0,63 = 0,4,$$

where the representation of parameters and physical variables in relative units is used. As a basic mode, the nominal load mode has been taken, according to the parameters of which the basic basis values are adopted (Table 2).

In this example, an equivalent three-phase load of 100 kW is realized with the parameters:

$$\cos \phi_l = 0,707; \quad z_l = \frac{3U_{nom}^2 \cos \phi_l}{P_l R_B} = \frac{3 \cdot 0,707 \cdot 220^2}{100 \cdot 10^3 \cdot 0,257} = 4; \tag{31}$$

$$r_l = z_l \cos \phi_l = 2,83; \quad l_l = z_l \sin \phi_l = 2,83.$$

The filter used in the load circuit is approximately tuned to cancel out 5–7 harmonics and has the parameters in relative units  $l_\pi = 0,286$ ,  $c_\pi = 3,88$ . Reproduction of the static mode with the given

Table 2  
The parameters of the basic regime and the basic values of the design scheme of the power plant.

Value	Designation	Formula	Value	Unit. am.
Active power of three-phase load	$P_l$		400	kW
Load power factor	$\cos \phi_l$		0,707	
Total power of three-phase load	$S_l$	$P_l / \cos \phi_l$	566	kVA
Angular Frequency of voltage	$f_1$		50	Hz
The effective value of phase voltage	$U_l$		220	V
The effective value of the phase current	$I_l$	$S_l / (3 U_l)$	857	A
Basic voltage	$U_B$	$\sqrt{2} \cdot U_l$	311	V
Basic current	$I_B$	$\sqrt{2} \cdot I_l$	1212	A
Basic angular frequency	$\omega_B$	$2\pi f_1$	314,1593	1/s
The basic angle of rotation	$\theta_B$		1	

Table 3  
Integral characteristics of the load channel after the filter in relative units.

$I_{effload}$	$U_{effload}$	$\cos \phi_{load}$	$S_{elload}$	$S_{el1load}$	$P_{elload}$	$Q_{1load}$	$Q_{2load}$	$k_{mload}$	$k_{sload}$	$k_{2load}$
0,22	0,7148	0,709	0,4717	0,408	0,289	0,288	0,236	0,614	0,709	0,8655

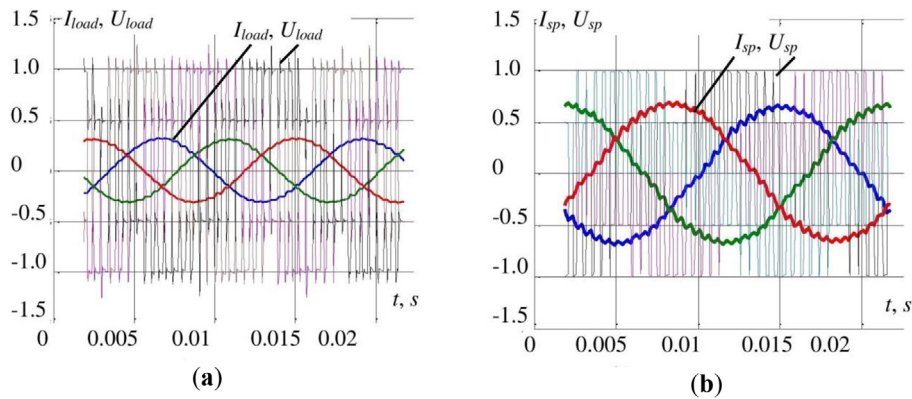


Fig. 5. Calculation diagrams of the currents and voltages of the load phases before the filter (a) and stator of the tidal machine in the operating mode of the pump motor (b).

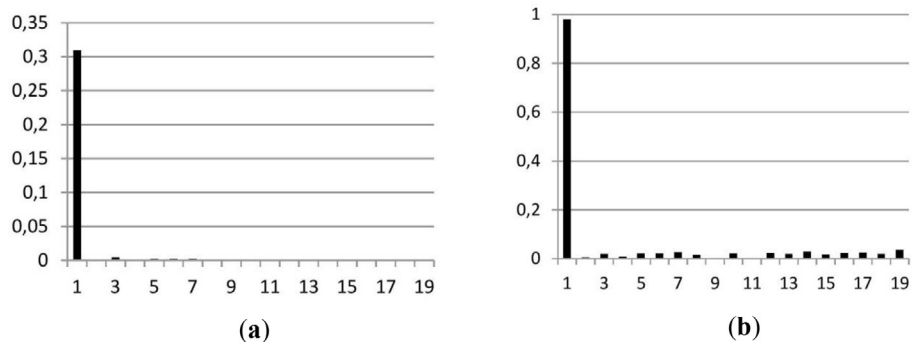


Fig. 6. The calculated spectra of the phase current harmonics (a) and the load voltage (b) in the static mode in relative units.

data has given a combination of indicators (Table 3). They show the effective implementation possibility of this and other operation modes of the autonomous power plant complex. Fig. 5 shows the calculated phase and load stress diagrams in the static mode under consideration. In the PWM algorithm, a clock frequency of 18 kHz and a modulation frequency of 1,8 kHz have been applied.

Fig. 6 shows the spectra of current harmonics and load voltages in the mode under consideration.

## 5. Conclusions

A mathematical model of a complex of an autonomous power plant built on the basis of a tidal aggregate and using other sources as a backup has been worked out. Efficient algorithms for mapping the functioning of electric machine aggregates complete with power electronic converters of electric energy parameters have been applied.

The detailed analysis possibility of various operating modes of the units, including the functioning of the tidal aggregate by the turbine and the pump, is illustrated.

The analysis of static and dynamic modes of operation of a power plant and its separate structures on the basis of computer modeling of deterministic and random processes of functioning makes it possible to obtain the necessary information for the selection of technical solutions for the development of energy efficient local power supply systems.

## Funding

This research was funded by the state task programme in the sphere of scientific activity of the Ministry of Science and High Education of the Russian Federation (project No. 5.4568.2017/6.7 and No. 13.2078.2017/4.6) and grant of the President of the

Russian Federation for state support of the leading scientific schools of the Russian Federation (NSh-2685.2018.5).

## Conflicts of interest

The authors declare that they have no conflict of interest.

## References

- Aboul-Seoud, T., Sharaf, A., A novel Dynamic Voltage Regulator compensation for a stand alone tidal energy conversion scheme, in: IEEE Electrical Power & Energy Conference 2010, Halifax, NS, Canada, 1–6, doi: 10.1109/EPEC.2010.5697210.
- Aboul-Seoud, T., Sharaf, A., Utilization of the Modulated Power Filter Compensator scheme for a grid connected rural hybrid wind/tidal energy conversion scheme, in: IEEE Electrical Power & Energy Conference 2010, Halifax, NS, Canada, 1–6, doi: 10.1109/EPEC.2010.5697211.
- Baykov, A.I., Dar'enkov, A.B., Sosnina, E.N., 2018. Simulation modeling of wind-diesel power station. Russian Electr. Eng. 3, 26–33. <https://doi.org/10.3103/S1068371218030033>.
- Bernshtein, L.B., Silakov, V.N., Gelfer, S.L., 1987. Tidal power plants; Energoatomizdat; Moscow, Russia, 296.
- Bierhoff, M.H., Fuchs, F.W., 2008. DC-link harmonics of three-phase voltage source converters influenced by the pulsewidth-modulation strategy – an analysis. IEEE Trans. Ind. Electron. 55, 2085–2092. <https://doi.org/10.1109/TIE.2008.921203>.
- Contestabile, P., Ferrante, V., Vicinanza, D., 2015. Wave energy resource along the Coast of Santa Catarina (Brazil). Energies 8, 14219–14243. <https://doi.org/10.3390/en81212423>.
- Devolder, B., Stratigaki, V., Troch, P., Rauwoens, P., 2018. CFD simulations of floating point absorber wave energy converter arrays subjected to regular waves. Energies 11, 641. <https://doi.org/10.3390/en11030641>.
- Ellabban, O., Abu-Rub, H., Blaabjerg, F., 2014. Renewable energy resources: current status, future prospects and their enabling technology. Renewable Sustainable Energy Rev. 39, 748–764. <https://doi.org/10.1016/j.rser.2014.07.113>.
- Tidal Energy. Technology Brief. IRENA Ocean Energy Technology Brief, 3 June 2014, 34.
- Falnes, J., 2007. A review of wave-energy extraction. Mar. Struct. 20, 185–201. <https://doi.org/10.1016/j.marstruc.2007.09.001>.
- Ocean Energy Forum. Draft Ocean Energy Strategic Roadmap Building Ocean Energy For Europe; Technical Report; European Commission: Brussels, Belgium, 2015.

- Ghefiri, K., Bouallègue, S., Haggège, J., Garrido, I., Garrido, A. Firefly algorithm based-pitch angle control of a tidal stream generator for power limitation mode. IC ASET 2018, Hammamet, Tunisia, 387–392, doi: 10.1109/ASET.2018.8379887.
- Gorev, A.A. Transient Processes of a Synchronous Machine; State Energy Publishing House: Leningrad-Moscow, Russia, 1950, 552.
- Gorji-Bandpy, M., Azimi, M., Jouya, M., 2013. Tidal energy and main resources in the Persian Gulf. *Distrib. Generation Alternative Energy J.* 82, 61–77. <https://doi.org/10.1080/21563306.2013.10677551>.
- Ivannikova, E.M., Sister, V.G., Vasilenko, A.P., Koltsova, E.S., Ivannikova, Y.M., 2015. Renewables in the Russian Federation and support of the state. *Alternative Energy Ecol.* 17 (18), 172–175. <https://doi.org/10.15518/isjaee.2015.17-18.028>.
- Khan, S.S., Tedeschi, E., 2017. Modeling of MMC for fast and accurate simulation of electromagnetic transients: a review. *Energies* 10, 1161. <https://doi.org/10.3390/en10081161>.
- Kocaman, A.S., Abad, C., Troy, T.J., Huh, W.T., Modi, V.A., 2016. stochastic model for a macroscale hybrid renewable energy system. *Renewable Sustainable Energy Rev.* 54, 688–703. <https://doi.org/10.1016/j.rser.2015.10.004>.
- Li, Y., McCalley, J.D., 2015. Design of a high capacity inter-regional transmission overlay for the US. *IEEE Trans. Power Systems* 30, 513–521. <https://doi.org/10.1109/TPWRS.2014.2327093>.
- Li, X., Wang, H., Zhao, H., Bao, H. Numerical simulation of the viscous flow around duct of tidal turbine, in: International Conference on Electrical and Control Engineering 2011, Yichang, China, 1637–1640, doi: 10.1109/ICECENG.2011.6058396.
- Maevskiy, O.A. Power characteristics of gate converters; Energiya: Moscow, Russia, 1978, 320.
- Maheshwari, Z., Ramakumar, R., 2017. Smart Integrated Renewable Energy Systems (SIREs): a novel approach for sustainable development. *Energies* 10, 1145. <https://doi.org/10.3390/en10081145>.
- Moghadas, A., Sarwat, A., Guerrero, J.M., 2016. A comprehensive review of low-voltage-ride-through methods for fixed-speed wind power generators. *Renewable Sustainable Energy Rev.* 55, 823–839. <https://doi.org/10.1016/j.rser.2015.11.020>.
- Mustafa, Sh.S., Misron, N., Lutfi, O.M., Tsuyoshi, H., 2017. Power characteristics analysis of a novel double-stator magnetic geared permanent magnet generator. *Energies* 10, 2048. <https://doi.org/10.3390/en10122048>.
- Powell, K.M., Rashid, Kh., Ellingwood, K., Tuttle, J., Iverson, B.D., 2017. Hybrid concentrated solar thermal power systems: a review. *Renewable Sustainable Energy Rev.* 80, 215–237. <https://doi.org/10.1016/j.rser.2017.05.067>.
- REN21. Renewables 2017 Global Status Report in perspective. Renewable Energy Policy Network for the 21st century, 2017, 43.
- Renzi, E., Dias, F., 2013. Hydrodynamics of the oscillating wave surge converter in the open ocean. *Eur. J. Mech.-B/Fluids* 42, 2–10. <https://doi.org/10.1016/j.euromechflu.2013.01.007>.
- Tekobon, J., Chabour, F., Nichita, C., Development of HILS emulator for a Hybrid Wind – Tidal Power System. CISTEM 2016, Marrakech, Morocco, 1–8, doi: 10.1109/CISTEM.2016.8066821.
- Twidell, J., Weir, T., 2015. *Renewable Energy Resources*. Routledge, London and New York, 784. ISBN 9780415584371.
- Vujacic, M., Hammami, M., Srndovic, M., Grandi, G., 2017. Theoretical experimental investigation of switching ripple in the DC-link voltage of single-phase H-bridge PWM inverters. *Energies* 10 (1189). <https://doi.org/10.3390/en10081189>.
- Wan, Y., Fan, Ch., Dai, Y., Li, L., Sun, W., Zhou, P., Qu, X., 2018. Assessment of the joint development potential of wave and wind energy in the South China Sea. *Energies* 11, 398. <https://doi.org/10.3390/en11020398>.
- Zhang, L., Li, M. Bond graph modeling and fault diagnosis of tidal turbine systems, in: Conference Chinese Control 2016, Chengdu, China, 6826–6831, doi: 10.1109/ChiCC.2016.7554431.